

Intergranular Microcracking due to Anisotropic Thermal Expansion in Calcite Marbles

Andrea SPAGNOLI^{1,a}, Anna Maria FERRERO^{1,b}, Maria MIGLIAZZA^{2,c}

¹ Department of Civil-Environmental Engineering & Architecture, University of Parma
Viale Usberti 181/A, 43124 Parma, Italy

² Dipartimento di Scienze della Terra "Ardito Desio", University of Milano
Via Mangiagalli 34, 20133 Milan, Italy

^a spagnoli@unipr.it, ^b annamaria.ferrero@unipr.it, ^c mariarita.migliazza@unimi.it

Keywords: bowing; crack propagation; fracture mechanics; marble; thermal cycles.

Abstract. *Marble slabs are frequently used as façade panels to externally cover buildings. In some cases bowing of such façade panels after a certain time of environmental exposure is experienced. The bowing is generally accompanied by a progressive reduction of strength. In the present paper, a theoretical model to calculate the progressive bowing and the thermal fatigue of marble slabs submitted to temperature cycles is presented. The model, developed within the framework of fracture mechanics, takes into account the mechanical microstructural characteristics of the marble as well as the actual cyclic temperature field in the material. The slabs are subjected to a thermal gradient along their thickness (due to different values of temperature between the outer and inner sides of the slab) as well as to thermal fluctuation on the two sides of the slab due to daily and seasonal temperature excursions. This thermal action causes a stress field which can locally determine microcracks due to decohesion of calcite grains. Stress intensification near the cracks occurs and leads to crack propagation in the slab. Such crack propagation under thermal actions is evaluated and the corresponding bowing is calculated.*

Introduction

Marble claddings are frequently used as façade panels to externally cover buildings. They are subjected to different actions that deteriorate the material, including: temperature (daily and seasonal excursions, through-thickness gradient), mechanical loads (wind, self-weight), chemical attacks (acid rain), humidity changes. Temperature may induce stresses due to thermal expansion (restraint effects of the anchorage system, nonlinear temperature fields, nonuniform/anisotropic thermal expansion). One visible phenomenon connected to deterioration of marble is bowing, which is characterised by permanent out-of-plane deflections. Bowing is generally accompanied by an overall reduction of strength which increases with increasing degree of bowing, while at the microstructural level of the material bowing is accompanied by a decohesion of calcite grains.

In order to understand the phenomenon of bowing in marble slabs, several experimental and theoretical studies [1-6] have been carried out, starting with the pioneering work of Rayleigh [7]. In situ measurements using a bow-meter [8] showed that the bowing of marble slabs, ranging from concave to convex shapes, is mainly dependent on the microstructure of the marble, the slab position, as well as on the fluctuation of temperature and moisture content. The determination of the overall mechanical behaviour of marble slabs on the basis of the aforementioned micromechanical phenomena might be performed within the framework of Linear Elastic Fracture Mechanics (LEFM) [9]. Accordingly, stress/strain state induced by cyclic thermal loading acting on the marble

slab can be determined along with the deflection of the slab due to both elastic bulk deformation and cracks.

In the present paper, following a recent work by the authors [10] a theoretical model to estimate the progressive bowing and the thermal fatigue of marble slabs submitted to temperature cycles is presented. The model, developed within the framework of LFM, takes into account the mechanical microstructural characteristics of the marble as well as the actual cyclic temperature field in the material. The slabs are subjected to a thermal gradient along their thickness (due to different values of temperature between the outer and inner sides of the slab) as well as to thermal fluctuation on the two sides of the slab due to daily and seasonal temperature excursions. This thermal action causes a stress field which can locally determine microcracks due to decohesion of grains. Stress intensification near the cracks occurs and leads to crack propagation in the slab. Such crack propagation under thermal actions is evaluated and the corresponding deflection (bowing) is calculated. Some examples are presented which show the strong influence of material microstructure on the degree of bowing.

Thermal Stresses in the Bulk Material

Attached to the slab of thickness h is a coordinate system with through-thickness axis x and longitudinal axis z . The kinematic assumptions are that of beam flexural theory (linear longitudinal strain along the beam height, the other strain components being null). A plane strain condition is assumed. The material is mechanically linear elastic, homogeneous and isotropic, while the thermal expansion is heterogeneous along the panel thickness. The resulting normal stress σ_z is

$$\sigma_z(x, t) = \frac{(1-\nu)E}{(1-2\nu)(1+\nu)} \varepsilon_z(x, t) - \frac{\alpha_z(x)E}{(1-2\nu)} \Delta T(x, t) \quad (1)$$

where $\Delta T(x, t)$ = temperature (variation with respect to a reference value) function of time t and space x obtained from an heat conduction analysis, E = Young modulus, ν = Poisson ratio, α_z = longitudinal thermal expansion coefficient, ε_z = longitudinal normal strain.

Beam theory leads to the following compatibility condition $\varepsilon_z(x, t) = A(t)x + B(t)$, where A and B , functions of time, are determined by applying the boundary conditions at the slab ends, which, in marble claddings, is dictated by the adopted anchorage system.

For a slab with clamped ends, ε_z is equal to zero and, hence, $A = B \equiv 0$. For a slab with hinged ends, the axial force and the bending moment are equal to zero. This yields the following expressions for A and B :

$$\begin{aligned} A(t) &= \frac{6}{h} \frac{1+\nu}{1-\nu} \left[\frac{2}{h} \int_0^h x \Delta T(x, t) \alpha_z(x) dx - \int_0^h \Delta T(x, t) \alpha_z(x) dx \right] \\ B(t) &= 2 \frac{1+\nu}{1-\nu} \left[2 \int_0^h \Delta T(x, t) \alpha_z(x) dx - \frac{3}{h} \int_0^h x \Delta T(x, t) \alpha_z(x) dx \right] \end{aligned} \quad (2)$$

It can be note that, if ΔT is a linear function of x , σ_z is equal to zero for mechanically and thermally homogeneous and isotropic case with hinged boundary conditions.

As it is well known [7], the thermal expansion of calcite grains is anisotropic. In the present model, where thermal expansion is assumed to be heterogeneous and hence the coefficient α_z is a function of the through-thickness coordinate x , the thermal expansion heterogeneity is linked to the aforementioned thermal anisotropy of calcite grains. Now let us assume that the thermal expansion of calcite grains is orthotropic (1-2 are the material thermal expansion axes, characterized by the coefficients α_1 and α_2 , respectively), the longitudinal thermal expansion coefficient along the z -axis α_z is obtained from

$$\alpha_z(x) = \alpha_1 \cos^4 \beta(x) + \alpha_2 \sin^4 \beta(x) \quad (3)$$

where β is the angle formed by the material thermal expansion axes with the longitudinal axis z . In particular β is the counterclockwise angle of 1 and z (Figure 1a).

In the light of the above, the thermal expansion heterogeneity (see $\alpha_z(x)$) is due to the different orientation (see $\beta(x)$) of the material thermal expansion axes of each grain. Therefore $\alpha_z(x)$ is hereafter assumed to be a stepwise varying function where a jump in such a function occurs at each calcite grain boundary. Assuming a geometrically simple grain arrangement for our model, we might have a stack of layers with different values of α_z in each layer, where the layer thickness might be taken as the calcite grain mean dimension d . In other word, the value of β changes each time the coordinate x attains a multiple value of d , see Figure 1a.

In the following, apart from the thermally homogeneous case, we assume a stack sequence of grains which is chessboard-like (a-b-a-b-a-), see Figure 1b; accordingly $\alpha_z(x) = \alpha_z^{(a)}$ [or $\alpha_z(x) = \alpha_z^{(b)}$] at points occupied by material “a” (or “b”). Also, we consider a random arrangement of thermal axis orientation in each grain.

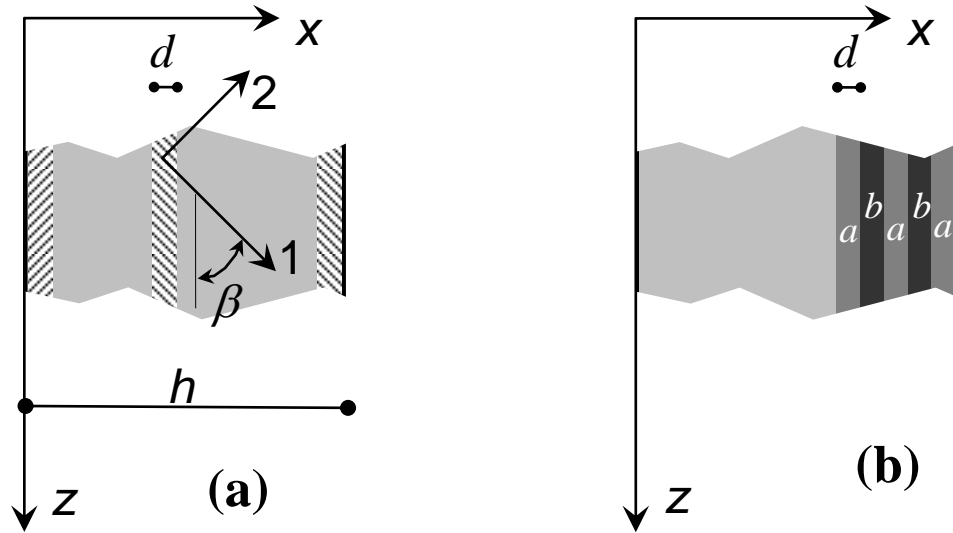


Figure 1. (a) Stack of grain layers along the slab thickness with different orientation of the thermal expansion axes 1-2; (b) Chessboard-like arrangement of grain layers.

Intergranular Microcracking

Under environmental conditions a diffuse cracking, mainly developing at the calcite grain boundaries, can take place at the external surface of the marble slab. Such a diffuse cracking can be incorporated in the present model to calculate the ensuing deflection of the slab due to thermal loading. Intergranular cracking due to decohesion of calcite grains are treated as equivalent multiple edge cracks. To this end a crack density parameter n , corresponding to a number of equivalent external edge cracks, can be defined. Assuming hence that intergranular cracking occurs, the crack density parameter can be correlated with the specific surface S_s of the grains (i.e. the total surface area of the grains per unit volume of material) as follows for a slab of length L (Figure 2a) [10]

$$n = \frac{S_s \cdot L}{2} \quad (4)$$

For instance, in the case of ideal cubic grains, the specific surface area S_s turns out to be equal to $6/d$ cm^2/cm^3 , that is, S_s is dependent on the grain size (note that typically calcite grain size d ranges from 100 to 500 μm). The shape of calcite grains is not accounted for in the present model, although

marble microstructures do present sometimes different geometric features (see the extreme cases of xenoblastic to homoblastic textures reported in Figure 2b).

Considering firstly an external edge crack submitted to the thermal stress σ_z acting in the slab, the Mode I Stress Intensity Factor (SIF) of the crack can be calculated using the theoretical 2D solution for point loads P (equal to $\sigma_z(a',t)da'$) acting on the crack faces at a depth a' ($a' = h - x$, with $0 \leq a' \leq a$) from the outer side and the superposition principle. According to the solution reported in Ref. [11], p. 71 we have

$$K_I(a,t) = \frac{2}{\sqrt{\pi a}} \frac{1}{\left(1 - \frac{a}{h}\right)^{3/2}} \int_0^a \sigma_z(a',t) \frac{G\left(\frac{a'}{a}, \frac{a}{h}\right)}{\sqrt{1 - \left(\frac{a'}{a}\right)^2}} da' \quad (5)$$

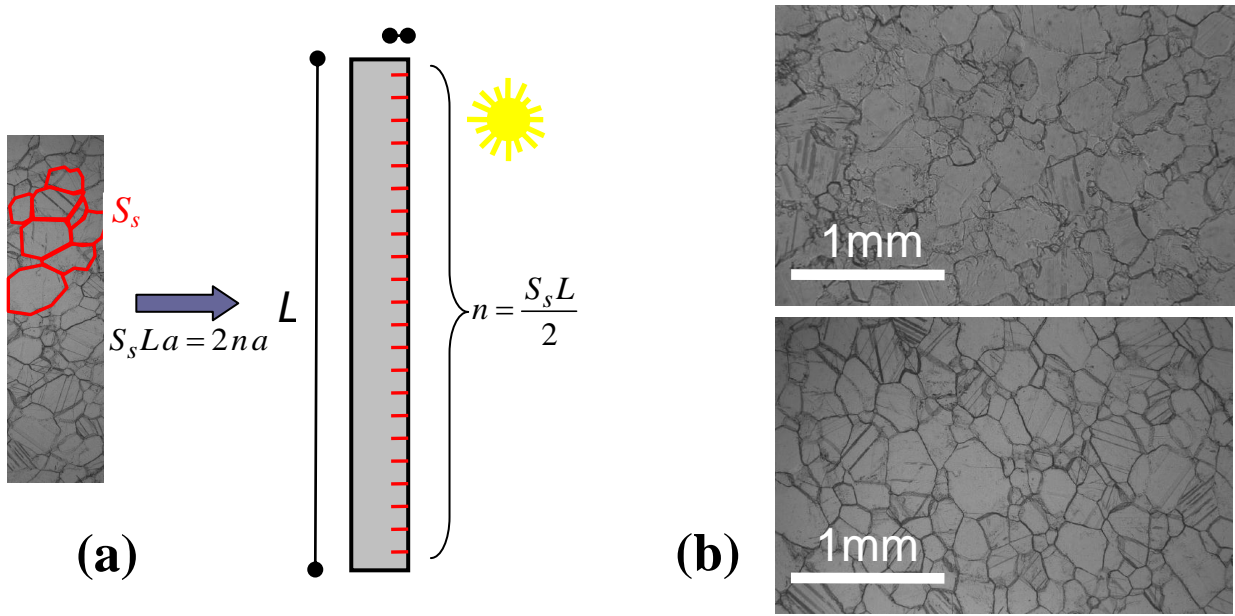


Figure 2. (a) Schematics on the intergranular equivalent cracking; (b) Two extreme cases of marble microstructure where the texture of calcite grains is evident (after Ref. [2]): xenoblastic texture where the grain boundaries are irregular (top), homoblastic texture where the grain boundaries are rather smooth (bottom).

Deflection as a Consequence of Microcracking

The presence of a single edge crack increases the compliance of the slab in comparison to the bulk counterpart. The corresponding deflection (positive outwards) at the centre of the slab can be worked out from energetic consideration [10]

$$f_{1crack}(a,t) = \frac{12}{Eh^2} \frac{L}{4} \int_0^a K_I^{(T)}(a',t) \sqrt{\pi a'} F\left(\frac{a'}{h}\right) da' \quad (6)$$

where $K_I^{(T)}(a,t)$ is the SIF, calculated according to Eq. 5, dependent on the temperature field $\Delta T(x,t)$, and the dimensionless function F refers to the pure bending solution (see Ref. [11], pp. 55-56). In the case of multiple microcracking on the external edge, the corresponding central deflection becomes

$$f_{ncracks}(a,t) = \frac{12}{Eh^2} \bar{z} \int_0^a K_I^{(T)}(a',t) \sqrt{\pi a'} F\left(\frac{a'}{h}\right) da' \quad (7)$$

where $\bar{z} = \frac{nL}{32}$ for clamped ends and $\bar{z} = \frac{nL}{8}$ for hinged ends of the slab.

Finally, the maximum value during a temperature cycle T of the crack-induced deflection for a crack of length a is given by $f(a) = \max_{t \in T} f_{nrcracks}(a, t)$.

Bowing as a Consequence of Microcrack Propagation

Since the slab is subjected to fluctuating temperatures, the consequent thermal stress σ_z acts as a cyclic load, producing in the microcracked material a periodic variation of SIF which in turn might be responsible of stable propagation of microcracks.

If one assumes that the empirical relation of Paris for fatigue crack growth is applicable to the present case of marble under thermal cycles [12], stable crack growth rate da/dN can be correlated with the variation of the SIF in the crack during a loading cycle $\Delta K_I(a)$ (where $\Delta K_I(a) = K_{I,max}(a) - K_{I,min}(a)$), namely [13] $da/dN = C\Delta K_I^m$ (C and m are material constants). Paris law can be integrated using a step-by-step procedure with a finite constant increment of crack length Δa and with an initial crack length a_0 (for instance equal to the mean dimension d of the calcite grains). At the first step, $K_I(a_0, t)$ and hence $\Delta K_I(a_0)$ is determined. Then the number of temperature cycles ΔN_1 needed to propagate the crack to a length $a_1 = a_0 + \Delta a$ is calculated. The procedure continues until a critical crack length a_c , according to a LFM failure criterion, is attained (for which the maximum SIF $K_{I,max}(a_c)$ during a loading cycle is equal to the fracture toughness of the material K_{IC}). Such a critical condition indicates unstable (instantaneous) crack propagation, and the corresponding number of cycles N_c gives the fatigue life (number of cycles to failure) of the slab.

Propagation of microcracks is an irreversible phenomenon, so that it is deemed to be reasonable to correlate the increment of slab deflection due to crack propagation to the slab bowing, which is characterized by permanent deflections. In other words, bowing $b(N)$ after a given number of cycles N is taken to be equal to $f[a(N)] - f(a_0)$.

Illustrative Example

We consider a typical case of a marble slab of thickness $h = 30\text{mm}$ and span L between anchorages equal to 0.6 m. The thermal cycles on the external and internal surfaces are described by in-phase sinusoidal functions. The temperature variation range is $\pm 11^\circ\text{C}$ and $\pm 9^\circ\text{C}$ on the external and internal surfaces, respectively. These temperature ranges are characteristic of diurnal temperature excursions in marble claddings in a Central Italy area [14].

The material parameters are [12]: $E = 52\text{ GPa}$, $\nu = 0.16$, $m = 4$, $C = 3 \times 10^{-4}$ (for da/dN expressed in m and ΔK_I in $\text{MPa m}^{0.5}$) $K_{IC} = 1.35\text{ MPa m}^{0.5}$ [12]. The mean size d of calcite grains is $200\ \mu\text{m}$ which corresponds for an ideal cubic tessellation to a specific surface of grain boundaries S_s equal to $300\ \text{cm}^2/\text{cm}^3$ and in turn, according to Eq. 4, to a crack density parameter $n = 9000$. From the literature we take $\alpha_1 = 25\ \mu\text{m}/\text{m}/^\circ\text{C}$, $\alpha_2 = -6\ \mu\text{m}/\text{m}/^\circ\text{C}$ [7]. In the present simulations, the initial cracking depth is taken as equal to d , namely $a_0 = 200\ \mu\text{m}$, and Δa is assumed to be equal to 1% of the current crack length a .

Let us assume a uniform Probability Density Function (PDF) for the orientation of thermal expansion axes of calcite grains with respect to the longitudinal axis z of the slab (Figure 1), that is

$$p(\beta) = \frac{1}{\pi} \quad \text{with } 0 \leq \beta \leq \pi \quad (8)$$

The weighted mean value of the longitudinal thermal expansion coefficient α_z becomes (see Eq. 3)

$$\mu[\alpha_z] = \int_0^\pi (\alpha_1 \cos^4 \beta + \alpha_2 \sin^4 \beta) p(\beta) d\beta = \frac{3}{8}(\alpha_1 + \alpha_2) \quad (9)$$

and the weighted variance is

$$\sigma^2[\alpha_z] = \int_0^\pi [(\alpha_1 \cos^4 \beta + \alpha_2 \sin^4 \beta) - \mu[\alpha_z]]^2 p(\beta) d\beta = \frac{0.417\alpha_1^2 - 0.736\alpha_1\alpha_2 + 0.417\alpha_2^2}{\pi} \quad (10)$$

The numerical values obtained from Eqs 9 and 10 for the marble under study are: $\mu[\alpha_z] = 7 \mu\text{m/m}/^\circ\text{C}$ and $\sigma[\alpha_z] = 11 \mu\text{m/m}/^\circ\text{C}$.

In the following simulations, as far as thermal expansion is concerned, we analyse 3 different cases: (i) homogeneous case where $\alpha_z(x) = \mu[\alpha_z]$; (ii) chessboard-like case (Figure 1b) where $\alpha_z^{(a)} = \mu[\alpha_z] + \sigma[\alpha_z]$ and $\alpha_z^{(b)} = \mu[\alpha_z] - \sigma[\alpha_z]$; (iii) random case where $\alpha_z(x) = \alpha_1 \cos^4 \beta(x) + \alpha_2 \sin^4 \beta(x)$ and $\beta(x)$ distribution follows the uniform PDF of Eq. 8. For case (iii), pseudo-random generation of $\beta(x)$ values is numerically performed. Since the statistical phenomenon is like a stochastic process (sequence of statistical values) a number of realizations are considered. In particular, three realizations of $\beta(x)$ sequence [termed random (1), random (2) and random (3)] are considered, bearing in mind that a much larger number would be needed to perform Monte Carlo-like simulations on the statistical outcome of the present model.

For the homogeneous case the normal stress distributions along the thickness of the slab at temperature peak for the hinged slab is nearly null, while, for the clamped slab, the stress values are relevant and they vary linearly along the thickness (for the clamped slab a number of thermal cycles of the order of 10^3 is needed to reach failure while for the hinged slab more the 10^{12} cycles are needed to reach failure). When thermal expansion of the material is treated as heterogeneous, both chessboard-like and random models (Figure 3) exhibit for the hinged slab, thermal stress values significantly higher than those in the homogeneous counterpart. The chessboard-like model produces an oscillating tensile/compressive stress distribution along the slab thickness, while the random model determines scattered values of stress but roughly with the same intensity as those related to the chessboard-like model.

Figure 4 shows bowing against number of thermal cycles for the hinged slab in the three thermal expansion cases being analysed. Figure 4a shows that an heterogeneous chessboard-like thermal expansion influences bowing evolution. Moreover, the random simulations (Figure 4b) indicate that the bowing evolution rate is significantly higher in comparison to the cases shown in Figure 4a. More in details, it can be noted that fatigue life of the slab is significantly reduced by the heterogeneous random distributions of thermal expansion along the slab thickness.

Conclusions

The paper proposes a theoretical model to estimate bowing in marble slabs subjected to thermal cycles. The model is based on LEFM concepts applied to marble slabs where grain decohesion due to surface damage can occur. The model is able to estimate the stress intensification near the crack tip and to compute the stress which leads to crack propagation in the slab. Such crack propagation under thermal actions is evaluated and the corresponding bowing is calculated. Some examples have been presented to show the strong influence of material microstructure on the degree of bowing. In particular, it has been shown that the evolution rate of bowing depends strongly on the degree of heterogeneity in the thermal expansion behaviour of the material. When a random distribution between calcite grains of the thermal expansion coefficient is considered (this being a reasonable description of the actual anisotropic thermal expansion of grains), the bowing evolution rate estimated according to the present model increases (and the fatigue life decreases) dramatically in

comparison to the results obtained with the rather idealized model with homogeneous or chessboard-like thermal expansion.

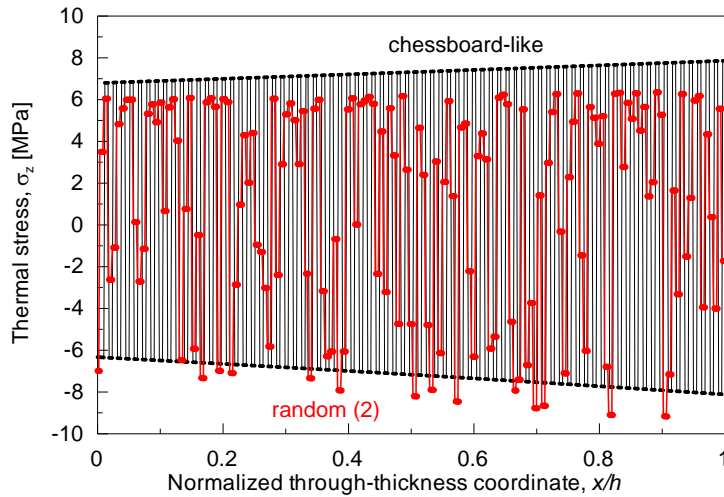


Figure 3. Thermal stress distribution along the thickness at $t = tP/4$ ($x = 0$ inner side) for chessboard-like model and random model (the 2nd realization of the stochastic process is reported) with hinged boundary conditions.

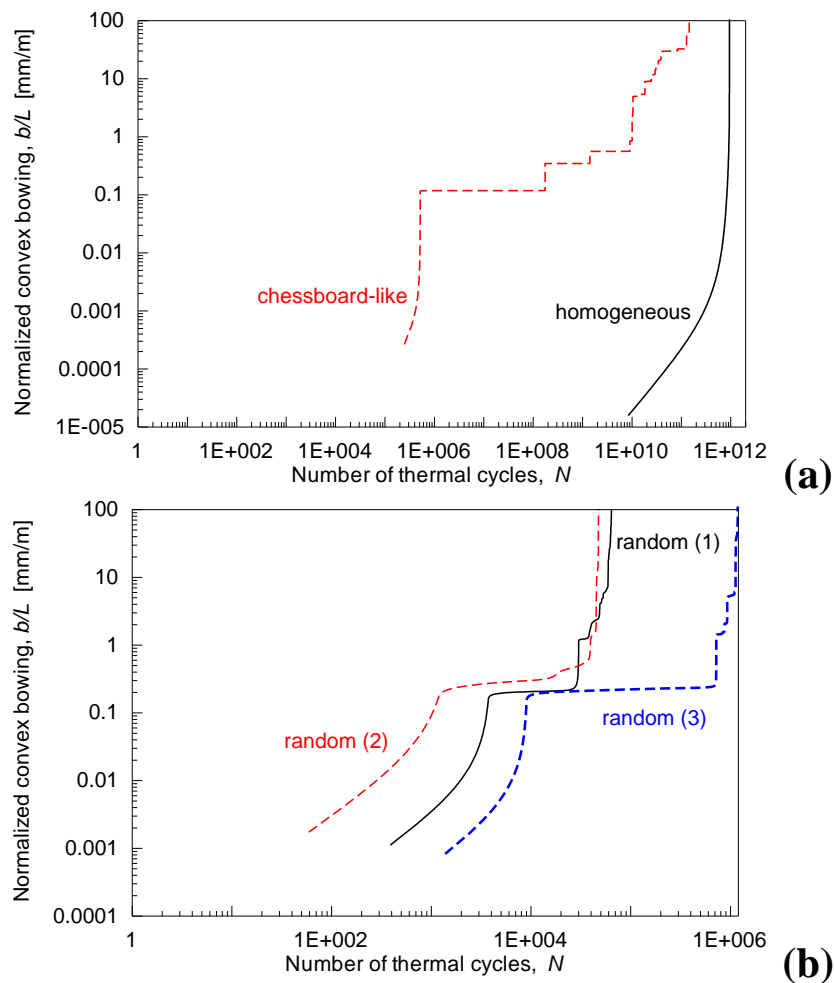


Figure 4. Bowing vs number of thermal cycles with hinged boundary conditions: (a) homogeneous and chessboard-like models; (b) three realizations of random model.

References

- [1] C. Widhalm, E. Tschegg and W. Eppensteiner. *ASCE Journal of Performance of Constructed Facilities* Vol. 10 (1996), pp. 5-10.
- [2] G. Royer-Carfagni. *International Journal of Rock Mechanics and Mining Science* Vol. 36 (1999), pp. 119-126.
- [3] B. Leiss and T. Weiss. *Journal of Structural Geology* Vol. 22 (2000), pp. 1737-1745.
- [4] S. Siegesmund, K. Ullemeyer, T. Weiss and E.K. Tschegg. *International Journal of Earth Sciences* Vol. 89 (2000), pp. 170-182.
- [5] A.M. Ferrero and P. Marini. *Rock Mechanics and Rock Engineering* Vol. 34 (2001), pp. 57-66.
- [6] C. Scheffzuk, S. Siegesmund and A. Koch. *Environmental Geology* Vol. 46 (2004), pp. 468-476.
- [7] A. Raileigh. *Proceeding Royal Society of London* Vol. 19 (1934), pp. 266-279.
- [8] A. Koch and S. Siegesmund. *Environmental Geology* Vol. 46 (2004), pp. 350-363.
- [9] K.T. Chau and J.F. Shao. *International Journal of Solids and Structures* Vol. 43 (2006), pp. 807-827.
- [10] A. Spagnoli, A.M. Ferrero and M. Migliazza. *International Journal of Solids and Structures* Vol. 48 (2011), pp. 2557-2564.
- [11] H. Tada H, P.C. Paris and G.R. Irwin. *The Stress Analysis of Crack Handbook*. Del Research Corporation, St.Louis (1985).
- [12] M. Migliazza, A.M. Ferrero and A. Spagnoli. *International Journal of Rock Mechanics and Mining Sciences* Vol. 48 (2011), pp. 1038-1044.
- [13] P.C. Paris, M.P. Gomez and W.P. Anderson. *The Trend in Engineering* Vol. 13 (1961), pp. 9-14.
- [14] A.M. Ferrero, M. Migliazza and A. Spagnoli. *Construction and Building Materials* Vol. 23 (2009), pp. 2151-2159.